MASTER SN CURVE METHOD FOR SHORT FIBER COMPOSITES- THEORY AND EXPERIMENTAL VALIDATION

Atul Jain[a,b*], Jose Manuel Veas[b], Stepan V. Lomov[b], Yasmine Abdin[b], Stefan Straesser[a], Wim Van Paepegem[c], Ignace Verpoest[b]

[a]*LMS International- A Siemens Business Interleuvenlaan Leuven, Belgium*
[b]*Department of Metallurgy and Materials Engineering, KU Leuven, Belgium*
[c]*Department of Material Science and Engineering, Ghent University, Belgium*
**atul.jain@lmsintl.com atul.jain@student.kuleuven.be*

Keywords: Fatigue, multi-scale damage, SN curves, mean field homogenization

Abstract

Typical short fiber composites components have a different statistical distribution of orientation of fibers at different points leading to different material mechanical and fatigue behavior at different points. For a component-sized calculation, each point in the FE model is the center of a Representative Volume Element (RVE) where the static and fatigue properties must be known. A hybrid multi-scale method of predicting the SN curve for every point in a short fiber composite is presented. This method is based on the assumption that the stiffness degradation curves of similar RVE must be similar. An extensive test program was undertaken to study the fatigue behavior of short fiber composites and validate the concept of the Master SN curve. Master SN curve was found to be in excellent match with the experimental results.

1. Introduction

Good specific properties and relative ease for large scale manufacturing make random fiber reinforced composites (RFRC) very attractive for a wide range of industries specially the automotive industry. For the manufacturing of RFRC, a range of different processes are available. Each process leads to a different statistical distribution of fibers at different points in the composite component, which in turn leads to different material properties, mechanical and fatigue behavior at different points, for different loading directions and types. There is quite a lot of literature describing the dependency of the SN curves of RFRC on the orientation distribution of the inclusion [1], [2] and [3], but the exact relation between the orientation and fatigue properties is unknown. Efficient fatigue simulation of RFRC is necessary for complete exploitation of the weight reduction potential of RFRC, a brief summary of the different challenges are available in [4]. For a component-sized simulation, each point in the FE model is the center of a Representative Volume Element (RVE), where each RVE has a given statistical distribution of orientation of fibers. The static and fatigue properties thus need to be estimated at every element. For an RVE, one can calculate the effective static properties of the composite by a number of different methods, for example the Mori-Tanaka formulation [5]. However, unlike elasticity there are no well understood and universally accepted formulations to describe fatigue, thus there is an absence of an analytical

method to predict the SN curve of a composite material. As a result one usually has to rely on test-based methods to estimate the SN curve of different RVE. Such methods depend on a number of tests on coupons with specific orientations which are usually time consuming and difficult to perform. The number of required tests can be reduced to 3 if one assumes that the orientation distribution of inclusions is only along one plane and that the length of all the inclusions is the same. Such assumptions are frequently made during fatigue simulation in industrial usage. Other approaches include a master SN curve approach where the "scaling" of SN curves is done on the basis of assuming proportionality between the Ultimate Tensile Stress (UTS) and fatigue strength, such an assumption is not always found to be true and besides there is an additional challenge of calculating correctly the ultimate tensile stress of a composite. More advanced methods of predicting S-N (stress-number of cycles to fail) behavior of reinforced plastics was by using fracture mechanics theory [6], this idea though attractive but has the limitation on depending upon a number of input parameter which are not usually available during fatigue simulation. To circumvent this problem we present in this paper a method to predict the SN curves of composites with different orientations and length distributions based on a hybrid multi-scale approach for scaling the SN curves; this proposed method involves both multi-scale-mechanics and tests.

2. Formulation of the Master-SN curve method

It is well known that composites suffer loss of stiffness when exposed to cyclic loading. We make an assumption that for short fiber composites having the same constituents (fiber and matrix) but different distribution of orientations, the loss of stiffness should be similar. In other words, RVE with different orientations, average aspect ratio, for a certain number of cycles the stress to failure is known to be different. But, the stiffness degradation curve must be similar. De Monte et al. [1] performed a series of fatigue tests in RFRC and noticed that while the fatigue strength of RFRC with different orientations at a given number of cycles varied from each other; the loss of stiffness trend was more or less the same. They reported that there was greater variation in the loss of stiffness curves in RFRC with the same fiber orientation as compared to RFRC with different orientations. In this approach, we attempt to model the stress-strain behavior including progressive damage of an RVE during the first cycle of loading. Homogenization is performed by the full-Mori Tanaka formulation [5] as opposed to a pseudo-grain discretized Mori-Tanaka formulation keeping in mind the better predictive ability of the Mori-Tanaka formulation for stresses in individual inclusions [7]. Initiation of fiber breakage and fiber matrix debonding and subsequent loss of stiffness is modeled. A broken fiber is replaced by two fibers half the original aspect ratio, fiber matrix debonding is treated by replacing an inclusion with an imperfect interface with a "perfectly bonded equivalent inclusion PBEI" as described by Jain et al.[8].

This proposed idea of scaling of SN curve is based on the damage operator that representing the loss of stiffness due to different damage events in the first cycle. Damage operator is defined by the following relation:

$$E_1 = E_0 (1 - d_n) \tag{1}$$

Where, E is the Young's modulus in the axial direction.
Each data point in the SN curve, gives information about number of cycles to failure (abscissa) and the strength to failure for the number of cycles (ordinate). Based on the available SN curve, the values of damage parameter are calculated for the ordinate points

corresponding to different values of abscissa. It is then assumed that for a given abscissa, different RVE may have different ordinates, but the values of damage parameter values corresponding to the abscissa are the same. Thus for different RVE, for a given abscissa, the ordinate is estimated by calculating the stress levels required to attain the same value of the damage parameter as was calculated from the input SN curve. Using this principle, the SN curves of different RVE can be estimated. A schematic representation of the Master SN curve scheme is shown in figure 1.

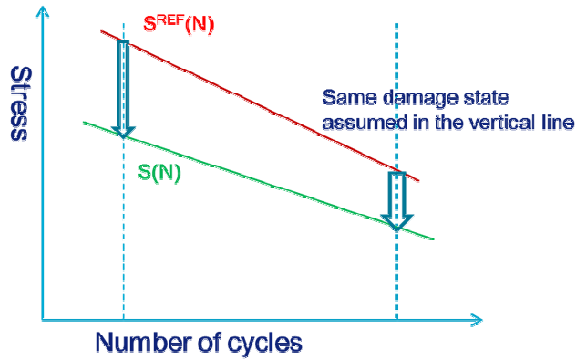

Figure 1 A schematic representation of the Master SN curve approach

3. Experimental tests and numerical validations

For validation of the Master SN curve approach, we performed a series of tests with injection molded BASF Ultradur B4040 G10 which has PBT matrix with 50% glass fiber weight fraction. Dog bone specimens are machined from injection molded plates 170mm×170mm with thickness 2mm. The thickness of the plate is chosen to be thin so that there is very little variation of orientation through thickness as the skin core effect commonly found in injection molding is minimized. The dimensions of the coupons are as per the test specimen according DIN ES ISO 527-2 Type 1B. Dog bone specimens are machined in three directions 0, 45 and 90 to the flow direction of the resin (figure 2d). In the remaining part of the paper, the orientation of the coupon is defined by the angle between the axis of coupon and the flow direction of the resin. Before the testing of the specimens the surfaces of the machined coupons are smoothened using a sand paper.

The manufacturing simulation of the injection molding is done using software Sigmasoft [9], the orientation distribution of the inclusions in the RVE was characterized by a second order orientation tensor [10]. The 2nd order orientation tensor is extracted and studied at three regions in the gauge length of the coupons and variation in the through thickness is estimated. It was seen that there was variation of less than 1% in the diagonal terms of the orientation tensor in the different positions of the gauge length and also in the thickness regions of the coupons. It was confirmed that we could perform our simulations reliably by treating the entire coupon as a single RVE. The 2nd orientation tensor, a_{ij} in the flow direction was found to be

$$a_{ij} = \begin{bmatrix} 0.81 & 0.018 & 0.137 \\ 0.018 & 0.11 & 0.004 \\ 0.137 & 0.004 & 0.079 \end{bmatrix} \quad (2)$$

The orientation distribution of the inclusions for the different coupons is generated by suitably rotating this second order orientation tensor.

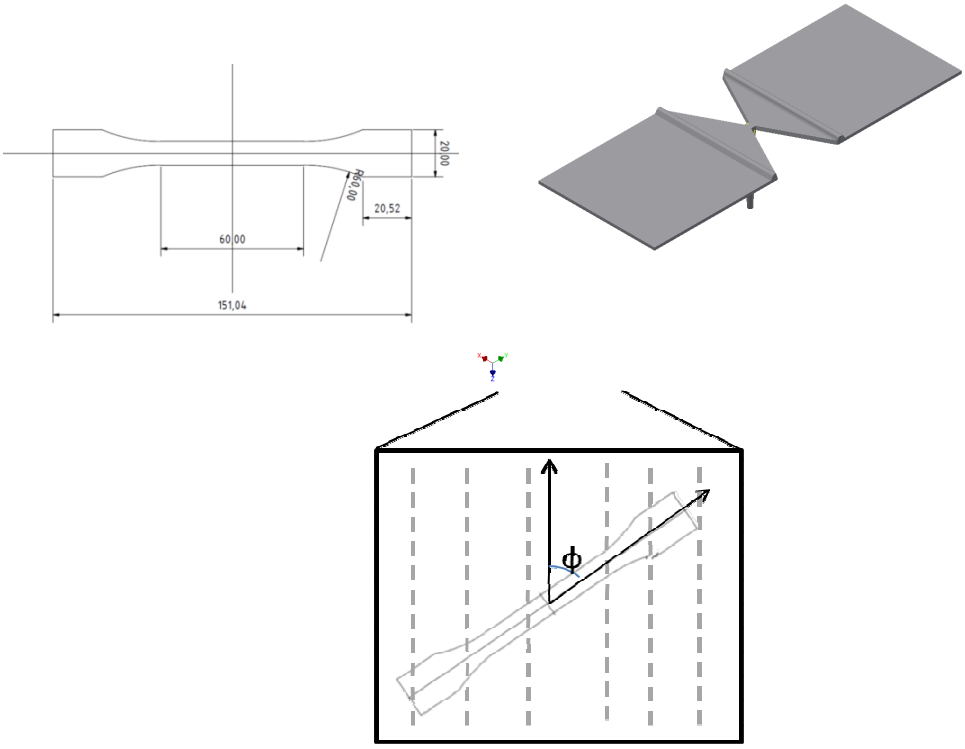

Figure 2: Figure 2a. The geometry of the dog bone specimen with dimensions in mm (top left); figure 2b plates used for injection molding (top right); figure 2c orientation designation of coupon (bottom right).

First, we performed a series of tensile tests to validate the micromechanical modelling including fiber matrix debonding and fiber breakage. After which fatigue tensile tests were carried out on a Schenck servo-hydraulic testing machine. The machine was equipped with a load cell of 10 kN. Tests were load controlled and a sinusoidal load function with constant amplitude was applied. Applied stresses were calculated dividing the applied load by the specimen net area, while the criterion to end the fatigue tests was complete specimen separation into two or more parts or no breakage until 10^6 cycles. The tests were performed at a load frequency of 10Hz; this was chosen such that the temperature measured on specimen surface did not exceed the room temperature by more than about 5deg C. Temperature monitoring was operated by a film type NiCr–Ni thermocouple, clamped on the central part of the specimen surface. We noticed that the rise of temperature in the surface of the specimen increases as the frequency of the applied load was increased and was about 3.3deg C at 10Hz, we decided not to go for higher frequencies to avoid resonance frequency problems with the machine. An extensometer was mounted on the specimens during the cyclic loading to keep track of the loss of stiffness during cyclic loading.

For the numerical simulation, software Converse[11] was used, special interfaces were created by PART Engineering GmbH in their software to allow access to certain results which are not a part of the standard output of software Converse. One by one each of the three experimentally derived SN curves was taken as input for the analysis and SN–curve predictions were compared with the remaining two experimentally derived SN curves. For

each validation we considered 3 experimentally derived points for cycles to failure close to 10^6, 10^5 and 1000 cycles. These data points are chosen such that for all the three coupons, there are some experimental points having similar number of cycles to failure. Thus, there are three sets of validations performed with three points each. For each of the calculations, we also simulated the SN curve for coupons with different orientations in between 0 and 90 to simulate the fatigue dependence on orientation of inclusions.

4. Results

Stress-strain curves derived from experiments are shown in figure 3. As expected, the modulus and failure strength of the coupons was found to be highest for the 0-deg coupon, followed by the 45 and 90deg coupons. The Young's modulus of the three coupons were found to be in the range of 16276-16296, 10366-10939 and 8450-8927 MPa respectively for the 0-deg, 45-deg and 90-deg coupons. Similarly the strength varied from 144-106, 71-64 and 49-44 MPa for the three coupons. Numerical simulation of the stress-strain curve by the Mori-Tanaka formulation and micromechanical modeling of fiber matrix debonding and fiber breakage led to good match with the experimental results particularly in the low stress region.

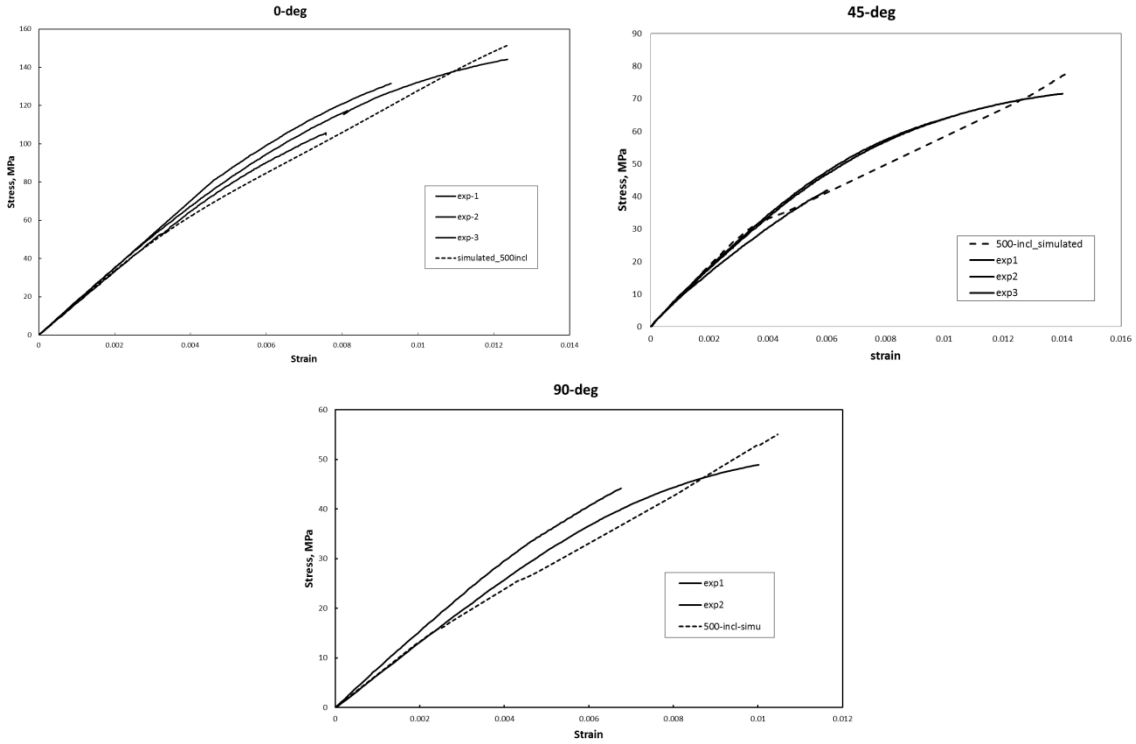

Figure 3: Stress-strain curves for 0, 45 and 90 deg. Both experimental results and simulated results are compared and reasonable match is found.

All the fatigue data was analyzed in the traditional method of plotting the stress amplitude against the number of cycles to failure in a double logarithmic scale. The data derived shows a linear relation in the double logarithmic plot. The k-ratio which is the inverse of the negative slope of the SN curve was found to be 14.70, 14.72 and 11.90 for the three set of coupons. The data seems to be in reasonable agreement with the existing literature, a summary of some available data and the k-ratio of the SN curve is listed in table 1. It is observed that there is strong dependency of the k-ratio on the fiber content of the RFRC, an increase in the fiber content leads to decrease in the value of k-ratio.

Ref.	Composite description	k-ratio
Test	50% GF with PBT	11.9-14.5
Gaier et al., 2008[3]	40% GF with PA 6T and filler	14-15.32
De Monte et al. , 2010[1]	35% GF with PA 6.6	15.4-18
Bernasconi et al., 2007[2]	17.5	19.80-22.94

Table1: A summary of the k-ratio of RFRC for composites with different weight fraction of inclusion. Note here that the k-ratio decreases as the proportion of glass fiber increases.

The SN curves of the RFRC were predicted using the proposed master SN curve approach. In the first case the experimental SN curve for the 0-degree coupon was taken as input and the data points starting as input was (1000000 cycles, 60 MPa), (134390 cycles, 69.89 MPa) and (1399 cycles, 90.76 MPa). The SN curves predicted for 45, 90 degree coupons were found to be in good agreement with the experimental results (figure 4a). In figure 4a the predicted SN curves are superimposed over the experimental results. In figure 4b the predictions of the Master SN curve for different orientations of the coupons are presented, note here that the orientation here refers to the angle at which the coupons were machined (figure 2d) and not the exact orientation of the inclusions inside the coupons.

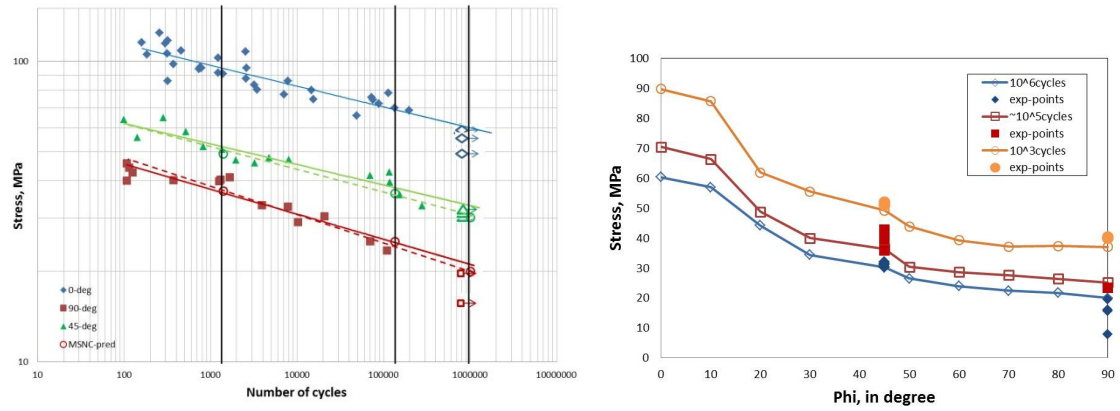

Figure 4: Figure 4a Validation of the master SN curve approach, the 0-degree coupon is taken as the input and the three vertical lines are the basis of the scaling. Dotted lines show the predicted SN curves while hollow symbols depict points predicted by the Master SN curve method. Figure 4b Points in the SN curve simulates for coupons with different orientations. Both experimental results and simulated results are compared and reasonable match is found.

In the second case of validation, the input SN curve is taken to be the 45 degree coupons. The data points taken for the validations are (1000000 cycles, 30.588 MPa), (118837 cycles, 39.51 MPa) and (1347 cycles, 50.93 MPa) (figure 5).

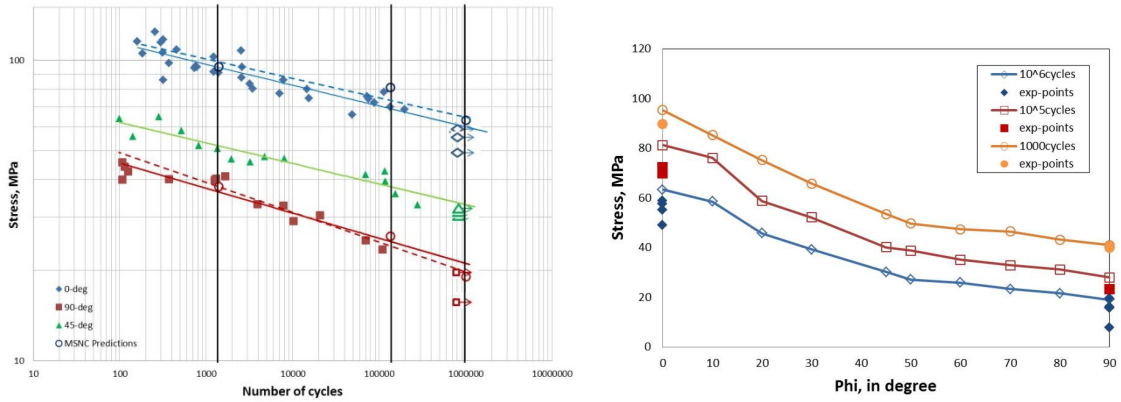

Figure 5: Figure 5a Validation of the master SN curve approach, the 45-degree coupon is taken as the input and the three vertical lines are the basis of the scaling. Dotted lines show the predicted SN curves while hollow symbols depict points predicted by the Master SN curve method. Figure 5b Points in the SN curve simulates for coupons with different orientations. Both experimental results and simulated results are compared and reasonable match is found.

Finally, the input SN curve is taken to be the 90 degree coupons. The data points taken for the validations are (1000000 cycles, 15.899 MPa), (109118 cycles, 23.389 MPa) and (1261 cycles, 39.86 MPa) (figure 6) predictions for the 45 and 0 degree coupons were derived.

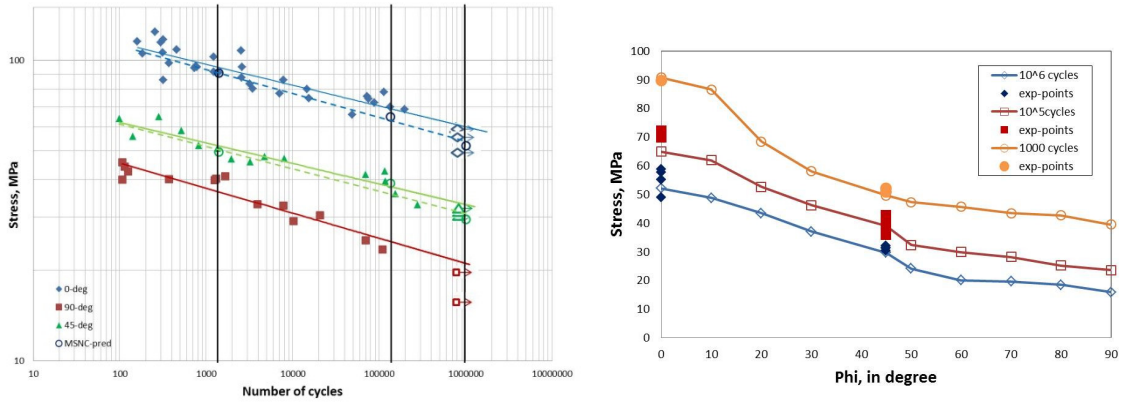

Figure 6: Figure 6a Validation of the master SN curve approach, the 90-degree coupon is taken as the input and the three vertical lines are the basis of the scaling. Dotted lines show the predicted SN curves while hollow symbols depict points predicted by the Master SN curve method. Figure 6b Points in the SN curve simulates for coupons with different orientations. Both experimental results and simulated results are compared and reasonable match is found.

In each of the three validation cases, good match is found with the experimental data irrespective of the SN curve is used as input. Master SN curve method predicts a strong dependency of fatigue on the orientation of the inclusions.

5. Conclusions and future outlook

A novel method of predicting the SN curve properties of RFRC at every point was presented in this paper. An experimental test program to validate the method was undertaken and it was seen that there is strong dependency of SN curve on the orientation distribution of the inclusions, but the slope of the SN curve is found to be more or less constant. The predictions of the Master SN curve approach was found to be in good agreement with the experimental test. The approach has furthermore been validated for different orientations of the input SN curve. Good accuracy is achieved irrespective of the orientation of the input SN curve. The

master SN curve approach could predict the orientation dependency of the SN curve. The input for such an analysis is only one input SN curve with no specific requirements to the configuration of the test coupon and elastic moduli of the matrix and fiber. This proposed methodology will be implemented in industrial software LMS Virtual.Lab Durability[12] part of Siemens PLM software [13]. An additional advantage of this method is that we have made no simplifying assumptions about the orientation and length distribution of inclusions. The fact that limited test data is required is a breakthrough in view of further industrial deployment of composites solutions in industry. It is vital that virtual simulation models can be created based on only a very limited amount of test data, as this will enable virtual optimization of the composites materials products in a more effective manner and at reduced costs. Besides predicting the SN curves at every point in the component, fatigue simulation must be able to account in an efficient manner for variable amplitude loading, multi-axiality and loss of stiffness during cyclic loading. These are seen as the logical next steps in the research program and are being currently explored.

6. Acknowledgement:

We gratefully acknowledge the support of IWT, Belgium for funding this research as a part of Baekeland project 100689 “Fatigue life prediction of random fiber composites using hybrid multi-scale modeling methods (COMPFAT)”. Part of the work presented here was performed by Jose Manuel Veas as a part of his Erasmus Master thesis project in KULeuven. PART Engineering GmbH provided special interfaces in their software Converse to give outputs necessary for the analysis presented in this paper.

References

1. De Monte, M., E. Moosbrugger, and M. Quaresimin, *Influence of temperature and thickness on the off-axis behaviour of short glass fibre reinforced polyamide 6.6-cyclic loading.* Composites Part a-Applied Science and Manufacturing. **41**(10): p. 1368-1379.
2. Bernasconi, A., et al., *Effect of fibre orientation on the fatigue behaviour of a short glass fibre reinforced polyamide-6.* International Journal of Fatigue, 2007. **29**(2): p. 199-208.
3. Gaier, C., et al., *Influence of Fiber Orientation, Temperature and Moisture on the Fatigue Behavior of Injection Molded Fiber Reinforced Thermoplastics.* Materials Testing-Materials and Components Technology and Application. **52**(7-8): p. 534-542.
4. Jain, A., et al., *Fatigue Life Simulation on Fiber Reinforced Composites - Overview and Methods of Analysis for the Automotive Industry.* SAE International Journal of Materials & Manufacturing, 2012. **5**(1): p. 205-214.
5. Mori, T. and K. Tanaka, *Average stress in matrix and average elastic energy of materials with misfitting inclusions.* Acta Metallurgica, 1973. **21**(5): p. 571-574.
6. Wyzgoski, M.G. and G.E. Novak, *An improved model for predicting fatigue S-N (stress-number of cycles to fail) behavior of glass fiber reinforced plastics.* Journal of Materials Science, 2008. **43**(8): p. 2879-2888.
7. Jain, A., et al., *Pseudo-grain discretization and full Mori Tanaka formulation for random heterogeneous media: Predictive abilities for stresses in individual inclusions and the matrix.* Composites Science and Technology. **87**: p. 86-93.
8. Jain, A., et al. *Model for partially debonded inclusions in the framework of mean-field homogenization*. in *Texcomp-11*. 2013. Leuven, Belgium.
9. Sigmasoft. *SIGMA Engineering GmbH, Aachen*. http://www.sigmasoft.de/ 2014 [cited.
10. Advani, S.G. and C.L. Tucker, *The use of tensors to describe and predict fiber orientation in short fiber composites.* Journal of Rheology, 1987. **31**(8): p. 751-784.
11. *PART Engineering*. http://www.part-gmbh.de/ 2014
12. *LMS International-A Siemens Business: Leading Partner in Test & Mechatronic Simulation*. http://www.lmsintl.com/simulation/virtuallab/durability 2014
13. *Siemens PLM software*. www.siemens.com/plm 2014